

Skyrme-Hartree-Fock-Bogoliubov calculation of nuclear structure properties in Pt isotopes

Dani Rose J Marattukalam[1] and A.K. Rhine Kumar[2]
Department of Physics, Cochin University of Science and Technology, Kochi - 682022, India.*

Abstract. In this work, we attempt to study the nuclear structure properties of the Pt isotopic chain in the framework of Hartree-Fock-Bogoliubov (HFB) theory. HFB theory is a Self-Consistent Mean Field (SCMF) model[1] that combines the nuclear mean-field Hartree-Fock (HF) theory and the Bardeen-Cooper-Schrieffer (BCS) theory that explains nuclear pairing correlations. We investigate the ground-state properties of the even-even isotopic chain $^{166-260}$Pt. These include the binding energy per nucleon, two-neutron separation energy, quadrupole deformation, proton, neutron and charge radii and neutron skin thickness. We also studied the dependence of neutron skin thickness on the temperature of the system. The code HFBTHO v2.00d[2] that solves the Skyrme HFB equations in the deformed harmonic oscillator basis was used to perform the calculations.

Communicated by Prof. S.D. Mahanti

1. INTRODUCTION

Hartree-Fock-Bogoliubov (HFB) theory is essentially a self-consistent framework generalizing the Hartree-Fock (HF) theory that describes the nuclear mean-field and the Bardeen-Cooper-Schrieffer (BCS) theory that explains nuclear pairing correlations [3]. HFB theory is considered a more general framework for the description of the nuclei than BCS theory as the single-particle wave functions and energies are specified beforehand in the BCS theory in terms of phenomenological mean-field potential, whereas HFB theory incorporates the complete HF theory with the relaxation of particle number conservation [4]. Also a single self-consistent theory was necessary while considering nuclei far from stability as the pairing correlations near the drip lines couldn't be accounted for merely as a residual interaction. In Hartree-Fock-Bogoliubov theory the state of the system is specified by two operators - the one-particle density matrix ρ which is the same as in Hartree-Fock theory and the pairing density matrix κ that describes the Cooper pairing effect [5]. In this work, we have studied the ground state properties of the even-even $^{166-260}$Pt isotopic chain by employing the HFB solver HFBTHO v2.00d [2].

*danimarattukalam95@gmail.com

2. THEORETICAL FRAMEWORK

In this section, we briefly describe the Skyrme-Hartree-Fock-Bogoliubov formalism. In second quantization, the general two-body Hamiltonian is written in terms of the particle creation and annihilation operators ($a^\dagger$, a) as:

$$H = \sum_{mn} e_{mn} a^\dagger_m a_n + \frac{1}{4} \sum_{mnpq} \bar{v}_{mnpq} a^\dagger_m a^\dagger_n a_p a_q \tag{1}$$

where $\bar{v}_{mnpq} = \langle mn|V|pq - qp\rangle$ are the anti-symmetrized two-body interaction matrix elements [6]. The Bogoliubov transformation [7] of the particles to quasi-particles [8] has the form:

$$\begin{pmatrix} \eta^\dagger \\ \eta \end{pmatrix} = \begin{pmatrix} U^T & V^T \\ V^* & U^* \end{pmatrix} \begin{pmatrix} a^\dagger \\ a \end{pmatrix} \tag{2}$$

U and V are the coefficients that transform the single-particle states (n) into quasi-particle states (μ). In the HFB calculations the nuclear ground-state wavefunction is defined as the quasi-particle vacuum i.e., action of quasi-particle annihilation operator on the wavefunction satisfies $\eta_\mu|\phi\rangle = 0$. We define the one-body density matrix ρ and pairing density matrix κ as follows:

$$\begin{aligned} \rho_{mn} &= \langle\phi|a^\dagger_n a_m|\phi\rangle = \sum_\mu V_{n\mu} V^*_{m\mu} \\ \kappa_{mn} &= \langle\phi|a_m a_n|\phi\rangle = \sum_\mu U_{m\mu} V^*_{n\mu} \end{aligned} \tag{3}$$

Performing the variation of energy in eq. (1) with respect to ρ and κ gives the HFB equations:

$$\begin{pmatrix} e + \Gamma - \lambda & \Delta \\ -\Delta^* & -(e+\Gamma)^* + \lambda \end{pmatrix} \begin{pmatrix} U \\ V \end{pmatrix} = E \begin{pmatrix} U \\ V \end{pmatrix} \tag{4}$$

where

$$\Gamma_{ij} = \sum_{kl} \bar{v}_{ikjl} \rho_{lk} \quad \text{and} \quad \Delta_{ij} = \frac{1}{2} \sum_{kl} \bar{v}_{ijkl} \kappa_{lk} \ . \tag{5}$$

The finite temperature HFB equations has a similar form except for the density matrices that now depend on the Fermi-Dirac occupation factor f_μ of the quasi-particle states μ [2].

$$\begin{aligned} \rho &= UfU^T + V(1-f)V^T \\ \kappa &= UfV^T + V(1-f)U^T \end{aligned} \tag{6}$$

The HFB energy can be written as:

$$E[\rho, \tilde{\rho}] = \int \mathcal{H}(\nabla) \lceil^{\ni} \nabla \tag{7}$$

where $\mathcal{H}(\nabla)$ is the local energy density as a function of nuclear densities and their derivatives with time-reversal symmetry. In the Skyrme-HFB approach, the total binding energy is given as a sum of the kinetic energy, the interaction energy between nucleons given by the Skyrme energy density functional, the pairing energy, the Coulomb energy and the correction arising from the spurious motion.

$$E = E_{kin} + \int \varepsilon_{Sk}\, d^3r + E_{pair} + E_{coul} - E_{corr} \tag{8}$$

For even-even nuclei, the Skyrme energy density functional takes the form [2]

$$\varepsilon_{Sk}[\rho] = C_t^{\rho\rho}[\rho]\rho_t^2 + C_t^{\rho\tau}[\rho]\rho_t\tau_t + C_t^{J^2}[\rho]\mathbf{J}_t^2 + C_t^{\rho\Delta\rho}[\rho]\rho_t\Delta\rho_t + C_t^{\rho\nabla J}[\rho]\rho_t\nabla\cdot\mathbf{J}_t \tag{9}$$

with τ_t and $\mathbf{J}_t$ being the kinetic energy density and the spin-current respectively. The coupling constants $C_t^{uu'}$ are functions of local isoscalar density $\rho_0(r)$ which are fitted to the data. We consider pairing correlations to arise from contact delta forces and hence the pairing energy density is given as

$$E_{pair} = \frac{1}{2}V_0\left[1 - V_1\left(\frac{\rho}{\rho_0}\right)^{\gamma}\right]\sum_q \tilde{\rho}_q^2 \tag{10}$$

where $\tilde{\rho}$ is the pairing local density with the index q labeling the neutron $(q = n)$ or the proton $(q = p)$. V_0 and V_1 are the coupling constants for pairing interaction.

The protons also experience a Coulomb potential due to their electric charges and hence the energy density will also have contributions from the Coulomb energy. The Coulomb energy has an exchange term apart from the usual direct term. The exchange term arises from the anti-symmetric nature of fermionic wavefunctions and is calculated using Slater approximation.

$$E_{Coul}^{dir} = \frac{e^2}{2}\iint d^3r d^3r' \frac{\rho_{ch}(\mathbf{r})\rho_{\mathbf{ch}}(\mathbf{r}')}{|\mathbf{r}-\mathbf{r}'|} \tag{11}$$

$$E_{Coul}^{ex} = -\frac{3}{4}e^2\left(\frac{3}{\pi}\right)^{1/3}\int d^3r \rho_{ch}^{4/3}(\mathbf{r}) \tag{12}$$

This form of the Energy Density Functional (EDF) can be used in the HFB equation obtained in eq. (4) to give the Skyrme-Hartree-Fock-Bogoliubov equations.

3. RESULTS

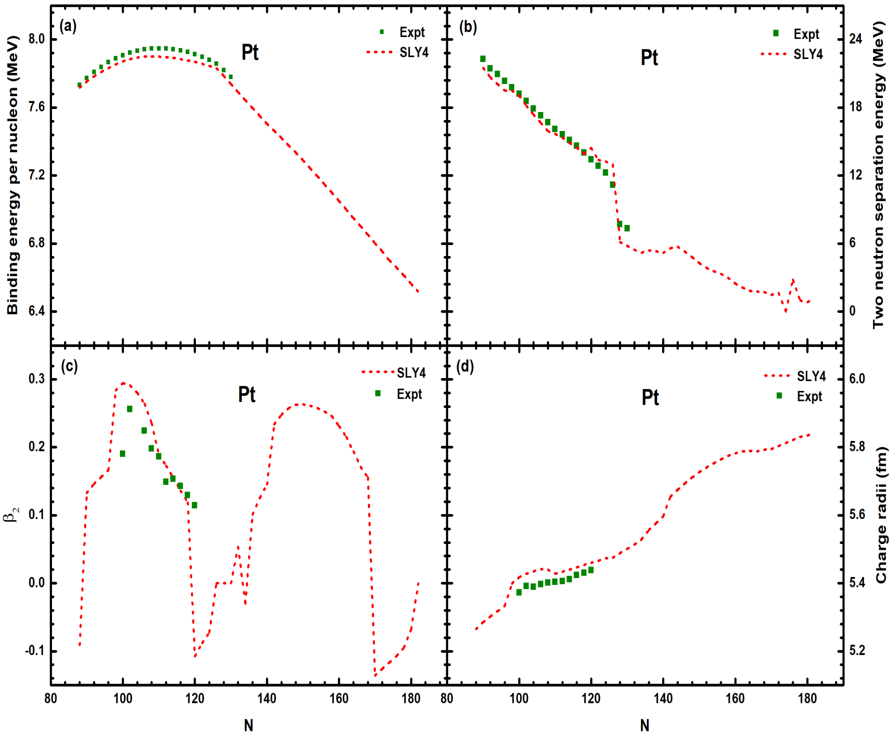

Figure 1. The (a) binding energy per nucleon, (b) two neutron separation energy, (c) the quadrupole deformation parameter, β_2 and (d) the charge radii calculated for the even-even isotopic chain $^{166-260}$Pt are plotted as a function of neutron number, N along with the experimental values [10–12].

Figure 1 shows the ground state properties of Pt isotopic chain, the binding energy per nucleon, the two-neutron separation energy, the quadrupole deformation parameter and the charge radii obtained using the Skyrme parameter set SLY4 [9]. We have used SLY4 parameterization as it was developed to give accurate results for neutron matter and nuclei far from stability. The calculated values are found to agree well with the experimental observations [10–12].

The binding energy per nucleon for the isotopic chains $^{166-260}$Pt are found to be within a range of 0.05 MeV of the experimental values. The difference is lower near the drip lines suggesting that SLY4 parameterization works well near the drip lines which was expected.

The two-neutron separation energy of a nucleus is defined as the energy required to separate two neutrons from the nucleus. A sharp decrease is found in the value of two-neutron separation energy at the magic number 126. Thus, it requires large energies to disrupt magic nuclei.

The quadrupole deformation β_2 of the nucleus is a general measure of its shape about the axially symmetric axis and determines the value of other parameters like quadrupole moment. The calculated values validate the fact that magic nuclei are generally spherical with $\beta_2 = 0$. This can be seen here for the magic neutron number 126.

The charge radius of a nucleus is defined as:

$$R_{ch} = \sqrt{R_p^2 + 0.64}\ . \tag{13}$$

This depends on the proton radius (R_p) and is usually a measure of the size of the nucleus. The charge radius indicates the proton distribution within the nucleus.

The proton radii and neutron radii are defined as the root mean square values of the respective density distributions.

$$< R_{\mathrm{q}}^2 >= \frac{\int r^2 \rho_{\mathrm{q}}(\vec{r}, T) d\vec{r}}{\int \rho_{\mathrm{q}}(\vec{r}, T) d\vec{r}} \tag{14}$$

Here, the densities are normalized to give the respective particle numbers,

$$\int \rho_q(\vec{r}, T) d\vec{r} = Q, \quad Q = Z, N; \text{ and } T \text{ represents the temperature.} \tag{15}$$

Thus, the proton and neutron radii are:

$$R_{\mathrm{n}} =< R_{\mathrm{n}}^2 >^{1/2} \qquad R_{\mathrm{p}} =< R_{\mathrm{p}}^2 >^{1/2} \tag{16}$$

The proton and neutron radii are calculated for the even-even isotopic chain $^{166-260}$Pt. Owing to the increasing number of neutrons as the mass number increases we also find an increase in the neutron radius.

The neutron skin thickness is an important parameter in nuclear physics, especially for exotic nuclei. This is defined as the difference between the neutron radii and the proton radii. We observe that the neutron skin depth increases with the neutron number and hence obtain an outer crust for heavier isotopes that is devoid of the protons, often called the neutron skin. So neutron-rich nuclei are often considered as an interesting tool, which connects finite and infinite nuclear matter. Here, we investigate the dependence of neutron skin thickness on the temperature. Fig. 2 shows the neutron skin thickness as a function of neutron number, N for different temperatures. The neutron skin thickness increases markedly with the increase in temperature. Hence, temperature plays a crucial role in neutron skin formation. This can be attributed to the occupation probabilities of the single-particle states around the Fermi level that varies with temperature [13]. As temperature increases higher unoccupied energy levels tend to be occupied causing larger proton and neutron radii. This leads to an increase in the neutron skin thickness.

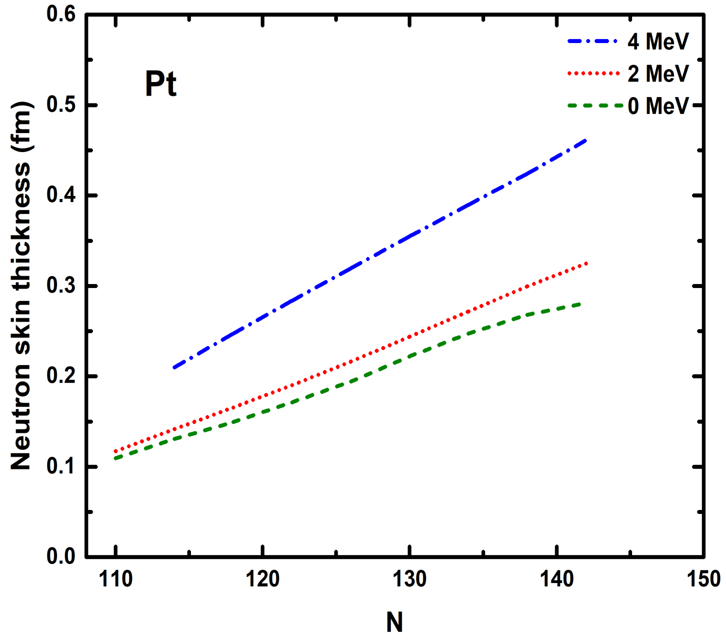

Figure 2. Neutron skin thickness as a function of neutron number, N at temperatures T = 0 MeV, T = 2 MeV and T = 4 MeV calculated for the even-even isotopic chain $^{188-222}$Pt.

4. CONCLUSION

We have calculated the ground-state as well as the excited state properties of the $^{166-260}$Pt isotopic chain using Skyrme-Hartree-Fock-Bogoliubov theory. Our results are in good agreement with the available experimental data. Further, we would like to extend our work to more systems, both finite nuclei and infinite nuclear matter, and the work is under progress.

ACKNOWLEDGEMENTS

A.K.R.K. acknowledges the financial support provided by the Department of Science and Technology (DST), India, via the DST-INSPIRE Faculty award.

References

[1] M. Bender, P.-H. Heenen, and P.-G. Reinhard, Rev. of Mod. Phys. **75**, 121 (2003).

[2] M. Stoitsov et al., Comp. Phys. Comm. **184**, 1592 (2013).

[3] J. Dobaczewski, H. Flocard and J. Treiner, Nucl. Phys. A **422**, 103 (1984).

[4] D.J. Rowe, *Nuclear Collective Motion: Models and Theory*, Methuen and Co. Ltd., London (1970).

[5] Mathieu Lewin and Sverine Paul, ESAIM: Math. Model. Numer. Anal. **48**, 5386 (2013).

[6] M. Stoitsov, J. Dobaczewski, W. Nazarewicz, and P. Ring, Comp. Phys. Comm. **167**, 43 (2005).

[7] N. N. Bogolyubov, Soviet Phys. Usp. **2**, 236 (1959).

[8] Walid Younes, Daniel Marc Gogny, and Jean-François Berger, *A microscopic theory of fission dynamics based on the generator coordinate method*, **950**, Springer International Publishing, Switzerland (2019).

[9] E. Chabanat, P. Bonche, P. Haensel, J. Meyer, and R. Schaeffer, Nucl. Phys. A, **635**, 231 (1998).

[10] M. Wang et al., Chin. Phys. C **45**, 030003 (2021).

[11] T. Belgya et al., *Handbook for calculations of nuclear reaction data*, RIPL-2. **IAEA-TECDOC-1506**, IAEA, Vienna (2006).

[12] I. Angeli and K. P. Marinova, At. Data Nucl. Data Tables **99**, 69 (2013).

[13] A. N. Antonov et. al., Phys. Rev. C **95**, 024314 (2017).